ACCURACY OF GAS - OIL RELATIVE PERMEABILITY FROM TWO-PHASE FLOW EXPERIMENTS

A.Skauge, G.Håskjold, T.Thorsen and M. Aarra
Norsk Hydro, N-5020 Bergen, Norway

Abstract
Gas - oil relative permeability of sandstone cores has been derived from constant rate and constant pressure gradient displacements, and also from drainage experiments by centrifuge. The paper discusses results from these types of measurements and the accuracy of estimated relative permeabilities. The relative permeabilities have been calculated from analytical methods neglecting capillary forces and by simulations of the experiments including capillary effects. The relative permeability is found to vary with viscous - capillary force balance, and the changes in relative permeability cannot fully be explained by capillary end-effects.

Introduction
The gas - oil relative permeability data reported in the literature are often calculated by neglecting capillary forces, and the errors in estimated relative permeabilities are generally not discussed. The objective of this paper has been to give recommendation as to methods and procedures for best estimates of gas - oil relative permeability. The errors made by neglecting capillary forces are discussed. Different experimental methods are analysed regarding the saturation range for reliable relative permeability estimates.

Gas-oil relative permeability is especially important for reservoirs with solution gas drive, gas cap expansion or gas injection. The accuracy of the laboratory measured relative permeability depends on the method applied and the experimental conditions. Gas-oil relative permeability is usually calculated from one or several of the mentioned methods[1]; unsteady state gas floods, constant pressure gradient gas injection, steady state measurements, centrifuge calculation of oil relative permeability. All the techniques for deriving gas-oil relative permeabilities have their strengths and weaknesses[1]. The main problem is the instability because of unfavourable mobility ratio and gravity segregation.

The low viscosity of the gas phase also gives low differential pressure in core flood experiments that contributes to inaccuracies in measurements and capillary end-effects. Usually gas-oil relative permeabilities are measured under conditions where not all assumptions used in deriving relative permeability data are valid.

Unsteady state gasfloods or gas injection is best performed in a gravity oriented experimental set-up, that is, by injecting gas from the top of a vertically oriented core. The rate applied is in most cases much higher than the gravity stable rate or critical rate as defined by Blackwell et al[2] and Dumore[3] .

$$u_C = (k\Delta\rho g)/\Delta\mu \qquad (1)$$

High rates have been applied to avoid capillary dominated flow regimes. The relative permeability can then be calculated from a JBN[4] - type procedure neglecting capillary forces. However, the frontal instability at higher rates causes viscous fingering and early gas breakthrough. Gas relative permeability may appear as miscible-type straight lines, while the oil relative permeability seems to be less effected by changes from capillary to viscous dominated flow[5].

Another approach has been to estimate gas-oil relative permeability from simulations including capillary pressure in core floods at gravity stable rates. This technique has the disadvantage that the differential pressure is very low and the relative permeability values appear to be less accurate. Measurement of in-situ saturation gives additional information about the frontal movement and thereby limit the confidence interval of the relative permeability curves.

The method of constant differential pressure has similarities to high-rate gas injection, as the purpose is to apply high differential pressure to eliminate the influence of capillary end-effects. The relative permeability is calculated assuming capillary forces can be neglected. Analysis of the constant differential pressure method shows that the core experiences a large variation in the ratio of viscous to capillary forces as described by the capillary number[6].

$$N_C = (\mu v)/\sigma \qquad (2)$$

The flow velocity increases during the experiment to maintain a constant dP. The influence of dynamic variation in flow regimes on the relative permeability is yet unsolved.
The capillary number may alternately be defined by:

$$N_C^* = (k_g \Delta P)/(\sigma L) \qquad (3)$$

where $N_c = N_c^* \; k_{rg}$ and $k_g = k_g\,(S_g = 1)$. The capillary number defined in equation 3 is constant during a constant differential pressure experiment. We have used eq.2 for long core gas injection and eq.3 for constant pressure gradient.

The steady state method has similar problems because of viscous instability at high rate and low differential pressure at low rates. In addition gravity segregation is always a question if the core is horizontal even when rotated during flow. An alternative approach is to measure k_{rog} by centrifuge[7]. This technique determines only the displaced phase relative permeability, but endpoint gas relative permeability may be obtained by gas flooding after the centrifuge experiment. Increasing the centrifuge rotational speed will change the gravity to capillary force balance, as described by the Bond number.

$$N_b = (kDrg)/s \qquad (4)$$

In centrifuge experiments the gravity acceleration can be exchanged with the centrifugal rotational speed and the rotational radius.

$$N_b = (kDrw^2\, r)/s \qquad (5)$$

In this paper we compare relative permeability for a gas drainage process calculated from both unsteady state, constant differential pressure and the centrifuge method. We also discuss the influence of capillary pressure on calculated relative permeabilities.

Experimental

The core material was outcrop sandstone cores, either Berea or Bentheimer. The permeability ranged from 100 to above 2,000 mDarcy. The fluid properties for each experiment are given in Table 1. All experiments were performed at room temperature. The physical properties of the core and initial saturation are shown in Tables 2 through 4.

The long core for gas displacement was mounted in viton shrink sleeve where aluminium foil and teflon were used to avoid gas diffusion from the core into the sleeve fluid. Three core flooding experiments were performed at gravity stable rate (rate $0.85q_c$, where q_c=11 ml/h), and two core floods at $1.43q_c$ and $8.0q_c$.

The experiments were performed at 52 bar backpressure and at room temperature. Measurements of in-situ saturation were performed with a X-ray scanning equipment. The apparatus has one X-ray source and it was anticipated that the water saturation did not change during the experiments. To increase accuracy in the measurements the oil phase was doped using 10% 1-iododecane in the oil phase. Before the experiments, scans were run with 100% methane, 100% oil and 100% water in the core. These readings were used for calculating the saturation profiles in the core.

The water was drained by a viscous oil (60cp) until an irreducible water saturation was obtained. The viscous oil was exchanged with decane and with methane-saturated decane (0.9)/1-iododecane (0.1) mixture. Saturation profile was established and used as a reference state for the core before the gas displacements. Between experiments, decane was injected to remove gas before injection of methane saturated decane (0.9)/1-iododecane (0.1) mixture. High pressure high precision pumps were used both to inject gas and to keep constant pressure at the production side. The produced fluids were monitored using an acoustic monitoring separator.

In centrifuge tests, oil relative permeability was derived by a technique similar to the method described by Hagoort[7]. The core samples were spun at overburden pressure in a J6B Beckman centrifuge with automatic camera reading of produced volumes. The maximum speed of the centrifuge is 3000 rpm. Measurements were made at several different rpm for each core plug. Physical data for the centrifuge experiments are reported in Table 4. The irreducable water saturation in the cores used for centrifuge and constant pressure gradient experiments was established by centrifuging at 3000 rpm. Saturation scans after drainage in the centrifuge show no end-effect.

Constant pressure gradient measurements were made by delivering gas to the core at a constant inlet pressure. The gas was injected from top of vertically oriented cores. The oil and gas production were monitored continuously. Table 3 gives data for the constant pressure gradient experiments.

Results and discussion

The rate effects on gas - oil relative permeability have been a controversial topic in earlier petroleum literature[1]. Effect of flow rate was observed for gas drainage in several studies reported in the literature, see ref. 1, page 92-97. Still, most gas drainage relative permeability data today is generated at high rate from arguments of reduced influence of capillary end-effects.

The three long core gravity oriented gas injection experiments were performed both below and above the critical rate as defined by equation 1. The oil production, Figure 1, shows earlier gas breakthrough when flow rates were above critical rate. Thus, higher gas injection rate is expected to increase gas relative permeability and reduces oil mobility. The relative permeabilities calculated by parameter estimation[7] including capillary pressure show higher gas relative permeability at high rate, while oil relative permeability was less changed, Figure 2. The gas front is clearly more dispersed at high rates, Figure 3. The high rate leads to instability and viscous fingering, because of increased capillary number and unfavourable mobility ratio. Simulations of the constant rate floods encountered difficulties in matching the high rate experiment.

Figure 4 shows the in-situ saturations after about 7 PV gas injected. The final liquid saturation shows the end-effect and the difference in saturations behind the front. The endpoint oil saturation is similar for all long core gas injections, but the internal saturation distribution differs to some degree. High gas injection rate reduces the end-effect, but this is compensated by the larger liquid saturation behind the front.

The centrifuge experiments reported in Table 4 have been used to calculate oil relative permeability by the method proposed by Hagoort[8]. The rotational speed was from 500 to 2500 rpm, and the corresponding Bond number varied from 10^{-7} to 10^{-3}. Figure 5 shows that oil relative permeability increases with centrifugal speed for all three classes of permeability. The oil relative permeability seems to be strongly dependent on centrifuge rotational speed. The question is then if this is only an end-effect or also an effect of the Bond number. Simulations of relative permeability from the centrifuge experiments using capillary pressure may explain this problem. Table 4 and Figure 7 shows that the remaining oil saturation vary with Bond number analog to capillary desaturation curves in as observed in an earlier publication[9]. Clearly, the centrifuge experiments are influenced by Bond number variations. If we analyse Figure 5 with regard to the minimum speed or Bond number required to obtain a speed insensitive relative permeability cores, respectively permeability, a critical Bond number can be defined, the $N_{B,Cr}$ is $6x10^{-5}$, $8x10^{-5}$, and $1x10^{-4}$ for low, medium and high.

Constant differential pressure experiments are shown in Figure 6. Relative permeability for the constant pressure gradient experiments has been calculated by a JBN[4]- analogue method. Changes in pressure gradients show less effect on relative permeability compared to the centrifuge k_r variations. Still the trends are that high permeability cores generally show increased relative permeability of both oil and gas at high differential pressure. The variation in capillary number, Figure 7, is much less than the Bond number variations for the centrifuge experiments, thus less change in relative permeability is expected.

Capillary pressure for the cores used in this study is reported in Figure 8. The influence of capillary pressure on calculated relative permeability from constant pressure gradient experiment is shown in Figure 9. Cores with permeability of about 200 mD were used in these experiments. The relative permeability measured under constant pressure gradient was found to be little affected when capillary pressure was taken into account, but the trend is that k_r is increased when calculated with capillary pressure. Figure 10 shows that oil relative permeability from centrifuge and constant pressure gradient overlap at 2500 rpm ($N_b = 10^{-3}$) and N_c^* in the range of 10^{-5}. Lower Bond number reduced the oil relative permeability.

Figure 11 compare oil relative permeability from the three different experimental techniques. The data was selected from the least capillary dominated centrifuge and constant pressure gradient experiments, while the gravity stable displacement was selected from the gas floods. As seen in Figure 11, the oil relative permeability deviates for the three methods, indicating variations with method or the force balance.

We have seen in Figure 5 that oil relative permeability vary with Bond number. Figure 12 displays centrifuge oil relative permeability for a low permeable core with and without account of capillary pressure. The oil relative permeability is increased at higher Bond number. If this is only an capillary end-effect, one set of oil relative permeability should fit all different rpm's or Bond number when capillary pressure is included in the simulation of the centrifuge experiments. However, as seen from Figure 12 simulations with capillary pressure at 500 and 2500 rpm gave very different oil relative permeability curves, indicating that oil relative permeability variations are not only end-effects, but may also change with the ratio of gravity-to-capillary forces, Bond number.

Figures 13-15 illustrate the statistical errors in estimated relative permeability from low and high rate long core gas injection, and from a constant pressure gradient experiment. The relative permeability is plotted against gas saturation in fraction of hydrocarbon pore volume. The covariance analysis shows that both gas and oil relative permeability are statistically well defined over large saturation ranges, except near the endpoint saturations.

Oil and gas relative permeability is generally lower in capillary dominated regimes. If gas - oil relative permeability should be estimated for a reservoir dominated by gravity drainage low rate gravity stable gas injection experiments is expected to give the best data representing the fliud flow description. High capillary number experiments could be more representative for the inflow into the production wells.

Conclusions

The long core gravity oriented displacements show more dispersed gas front and lower recovery efficiency at higher gas flow rate. However, the capillary end-effect is similar and seems less affected by

The relative permeabilities calculated by parameter estimation including capillary pressure show higher gas relative permeability at high rate, while oil relative permeability was less changed by flow rate.

Increased viscous or gravity forces generally have been found to give higher oil and gas relative permeability. In the centrifuge experiments the variation of k_{ro} with rotational speed was larger for the lower permeability cores. Similar results were observed for the constant pressure gradient measurements.
The covariance analysis have shown that both gas and oil relative permeability are well defined over large saturation ranges, except near the endpoint saturations.

Simulation of centrifuge experiments including capillarity still gave k_r that varied with rotational speed, indicating that analytical relative permeability variation with rpm can not be explained only by end-effect but seems also to be a dependency of the Bond number.

Acknowledgement
The authors acknowledge Norsk Hydro for permission to publish the paper.

Nomenclature

: viscosity (Pa.s)
: velocity (m/s)
: difference
: permeability (Darcy)
: velocity (m/s)
: interfacial tension (N/m)
: number (dimensionless)
: gravity (m/s^2)
: radius (m)
: rotational speed
: density (kg/m^3)
: length (m)
: saturation

subscripts
c : critical
st : stable
g : gas
rg : gas relative permeability
c : capillary
b : Bond

References

1. Honarpour, M., Koederitz, L., and Harvey, A.H. "*Relative Permeability of Petroleum Reservoirs,"* CRC Press, Boca Raton, Florida, 1986
2. Blackwell, J.T., and Terry, M.W.: "Factors Influencing the Efficiency of Miscible Displacement," *Trans*. AIME **216**, 1-8, 1959
3. Dumore, J.M.: "Stability Considerations in Downwards Miscible Displacements," *SPEJ* , 356-62, 1964
4. Johnson, E.F:, Bossler, D.P., and Naumann, V.O.: "Calculation of Relative Permeability from Displacement Experiments," *Trans*. AIME **216**, 370, 1959
5. Stalkup, F.I.: "*Miscible Displacement*," Monograph series, SPE, Richardson, 8, New York 1984.
6. Lake, L. W.: "*Enhanced Oil Recovery,"*, Prentice Hall, New Jersey, 1989.
7. Vignes, O.: "*Application of Optimization Methods in Oil Recovery Problems*" Ph.D. thesis, U. of Trondheim, 1993
8. Hagoort, J.: "Oil Recovery by Gravity Drainage," Soc. Petr. Eng. Journal, 139-149, June 1980
9. King, M.J., Falcone, A.J., Cook, W.R., Jennings, J.W., and Mills, W.H.: "Simultaneous Determination of Residual Oil Saturation and Capillary Pressure Curves Utilizing the Ultracentrifuge," SPE 15595, ATCE, New Orleans, Oct 1986.

Table 1 Fluid properties

	IFT, mN/m	oil density, kg/m3	oil viscosity, mPa.s	gas viscosity, mPa.s	gas density kg/m3
long core, 52 bar	10	782	0,58	0,02	36
centrifuge, 1bar	16	800	2,8	0,018	1
constant pressure gradient, 1bar	16	800	2,8	0,018	1

Table 2. Long core unsteady state experiments (*qc = 11 ml/h)

exp - core	L (cm)	PV (ml)	Kw (mD)	Qi (ml/h*)	Nc	Swi	Ko(Swi)	Sof	krg(Sof)
f1	60.65	143.4	240	0,85*qc	1.34E-08	0.23	240	0.249	0.18
f2	60.65	143.4	240	1,43*qc	2.26E-08	0.23	240	0.257	0.18
f3	60.65	143.4	240	8*qc	1.26E-07	0.23	240	0.262	0.28

Table 3. Constant pressure gradient experiments

exp - core	L (cm)	PV (ml)	Kw (mD)	dP, kPa	Nc*	Swi	Ko(Swi)	Sof	krg(Sof)
p1	6.39	13.85	133	19	3.55E-06	0.144	191	0.289	
p2	6.39	13.85	133	38	7.10E-06	0.144	191	0.26	
p3	6.39	13.85	133	57	1.06E-05	0.144	191	0.289	
p4	6.42	14	129	19	3.51E-06	0.146	190	0.319	
p5	6.42	14	129	38	7.03E-06	0.146	190	0.253	
p6	6.42	14	129	57	1.05E-05	0.146	190	0.25	
p7	6.42	14	129	75.84	1.40E-05	0.146	190	0.243	
p8	6.42	14	129	89.63	1.66E-05	0.146	190	0.246	0.89
p9	6.5	14.15	124	18.96	3.59E-06	0.148	197	0.286	
p10	6.5	14.15	124	37.92	7.18E-06	0.148	197	0.254	
p11	6.5	14.15	124	56.88	1.08E-05	0.148	197	0.254	
p12	6.5	14.1	125	18.96	3.61E-06	0.145	198	0.28	
p13	6.5	14.1	125	37.92	7.22E-06	0.145	198	0.262	
p14	6.5	14.1	125	56.88	1.08E-05	0.145	198	0.255	
p15	6.44	15.8	359	12	5.57E-06	0.104	478	0.294	
p16	6.44	15.8	359	22	1.02E-05	0.104	478	0.263	
p17	6.44	15.8	359	31	1.44E-05	0.104	478	0.269	0.85
p18	6.44	15.8	407	8.3	4.37E-06	0.101	542	0.335	
p19	6.44	15.8	407	16	8.42E-06	0.101	542	0.513	
p20	6.44	15.8	407	33	1.74E-05	0.101	542	0.266	0.60
p21	6.44	15.8	407	41.37	2.18E-05	0.101	542	0.25	0.69
p22	6.44	15.8	407	46.88	2.47E-05	0.101	542	0.247	0.75
p23	6.44	16.7	587	6.21	4.21E-06	0.111	698	0.329	0.55
p24	6.44	16.7	587	12.07	8.18E-06	0.111	698	0.308	
p25	6.44	16.7	587	18.13	1.23E-05	0.111	698	0.245	
p26	6.44	16.35	414	7.58	4.29E-06	0.104	583	0.315	
p27	6.44	16.35	414	15.17	8.58E-06	0.104	583	0.3	
p28	6.44	16.35	414	22.75	1.29E-05	0.104	583	0.263	0.72
p29	6.52	15.95	2.024	4.14	6.62E-06	0.044	1.667	0.273	
p30	6.52	15.95	2.024	6.89	1.10E-05	0.044	1.667	0.251	
p31	6.52	15.95	2.024	9.65	1.54E-05	0.044	1.667	0.229	
p32	6.52	15.95	2.024	12.41	1.98E-05	0.044	1.667	0.219	
p33	6.52	15.95	2.024	15.17	2.42E-05	0.044	1.667	0.213	
p34	6.53	15.2	2.017	4.14	6.72E-06	0.049	1.697	0.273	
p35	6.53	15.2	2.017	6.89	1.12E-05	0.049	1.697	0.243	
p36	6.53	15.2	2.017	9.65	1.57E-05	0.049	1.697	0.22	
p37	6.52	16.05	2.303	4.14	7.02E-06	0.037	1.768	0.293	
p38	6.52	16.05	2.303	6.89	1.17E-05	0.037	1.768	0.262	
p39	6.52	16.05	2.303	9.65	1.64E-05	0.037	1.768	0.249	
p40	6.52	15.55	2.029	4.14	7.02E-06	0.039	1.769	0.273	
p41	6.52	15.55	2.029	6.89	1.17E-05	0.039	1.769	0.238	
p42	6.52	15.55	2.029	9.65	1.64E-05	0.039	1.769	0.228	

Table 4. Centrifuge experiments

exp -core	L (cm)	PV (ml)	Kw(mD)	RPM	NB	Swi	Ko(Swi)	Sof	krg(Sof)
c1	6.5	14.15	124	457	6.27E-06	0.148	197	0.391	0.63
c2	6.5	14.15	124	557	9.32E-06	0.148	197	0.292	0.74
c3	6.5	14.15	124	737	1.63E-05	0.148	197	0.187	0.96
c4	6.5	14.15	124	971	2.83E-05	0.148	197	0.147	
c5	6.5	14.15	124	1.483	6.61E-05	0.148	197	0.092	
c6	6.5	14.1	125	457	6.30E-06	0.145	198	0.39	0.65
c7	6.5	14.1	125	737	1.64E-05	0.145	198	0.179	0.81
c8	6.5	14.1	125	971	2.85E-05	0.145	198	0.122	
c9	6.5	14.1	125	1.483	6.64E-05	0.145	198	0.093	
c10	6.39	13.85	133	2.518	1.85E-04	0.144	191	0.064	1.19
c11	6.42	14	129	2.518	1.84E-04	0.146	190	0.059	1.21
c12	6.44	15.8	262	557	1.51E-05	0.155	319	0.234	0.99
c13	6.44	15.8	262	699	2.38E-05	0.155	319	0.186	0.92
c14	6.44	15.8	262	997	4.83E-05	0.155	319	0.142	0.98
c15	6.44	15.95	316	699	2.85E-05	0.132	382	0.18	0.97
c16	6.44	15.95	316	997	5.79E-05	0.132	382	0.137	1.05
c17	6.44	16.7	587	457	2.22E-05	0.111	698	0.272	0.66
c18	6.44	16.7	587	557	3.30E-05	0.111	698	0.186	0.84
c19	6.44	16.7	587	699	5.20E-05	0.111	698	0.129	0.81
c20	6.44	16.7	587	971	1.00E-04	0.111	698	0.081	
c21	6.44	16.7	587	1.483	2.34E-04	0.111	698	0.046	
c22	6.44	16.35	414	457	1.86E-05	0.104	583	0.281	0.60
c23	6.44	16.35	414	699	4.34E-05	0.104	583	0.149	0.82
c24	6.44	16.35	414	971	8.38E-05	0.104	583	0.098	
c25	6.44	16.35	414	1.483	1.95E-04	0.104	583	0.064	
c26	6.44	15.8	359	2.518	4.62E-04	0.104	478	0.051	1.05
c27	6.44	15.8	407	2.518	5.24E-04	0.101	542	0.047	1.01
c28	6.52	15.95	2.024	456	5.28E-05	0.044	1.667	0.175	0.63
c29	6.52	15.95	2.024	557	7.88E-05	0.044	1.667	0.101	0.66
c30	6.52	15.95	2.024	737	1.38E-04	0.044	1.667	0.075	0.72
c31	6.52	15.95	2.024	997	2.53E-04	0.044	1.667	0.047	0.77
c32	6.52	15.95	2.024	2.507	1.60E-03	0.044	1.667	0.034	
c33	6.53	15.2	2.017	456	5.38E-05	0.049	1.697	0.156	0.64
c34	6.53	15.2	2.017	737	1.41E-04	0.049	1.697	0.06	0.78
c35	6.53	15.2	2.017	997	2.57E-04	0.049	1.697	0.033	0.78
c36	6.53	15.2	2.017	2.507	1.63E-03	0.049	1.697	0.013	
c37	6.52	16.05	2.303	456	5.60E-05	0.037	1.768	0.168	0.64
c38	6.52	16.05	2.303	2.507	1.69E-03	0.037	1.768	0.033	
c39	6.52	15.55	2.029	456	5.61E-05	0.039	1.769	0.152	0.62
c40	6.52	15.55	2.029	2.507	1.70E-03	0.039	1.769	0.014	

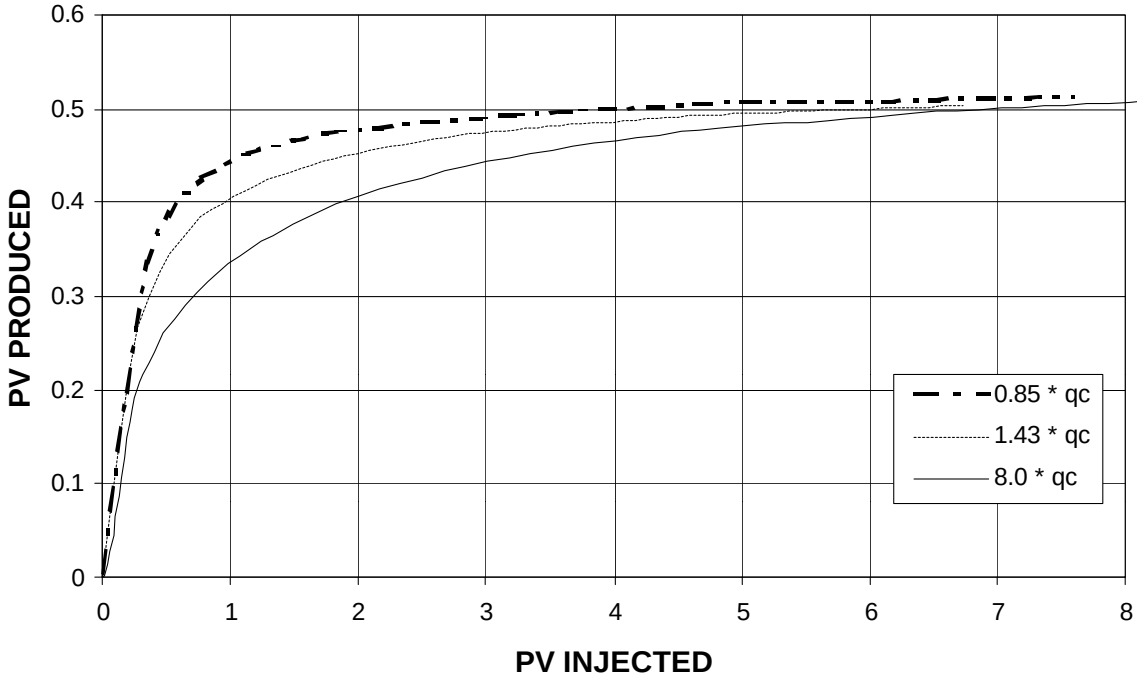

Figure 1. Oil production from long core gas injection.

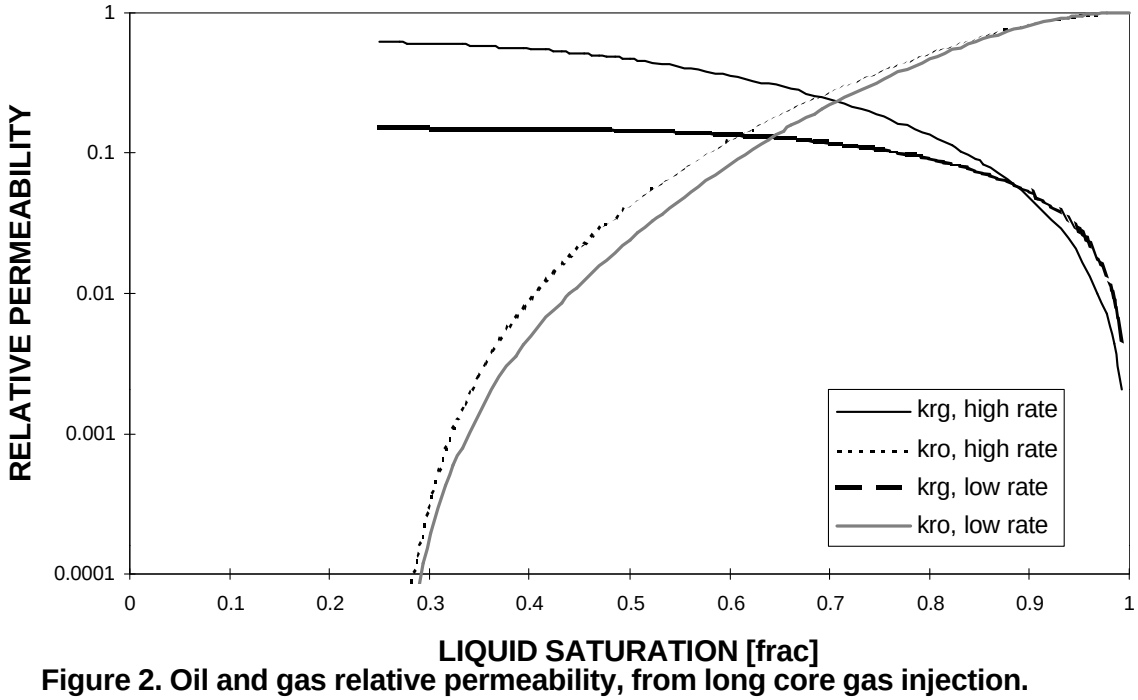

Figure 2. Oil and gas relative permeability, from long core gas injection.

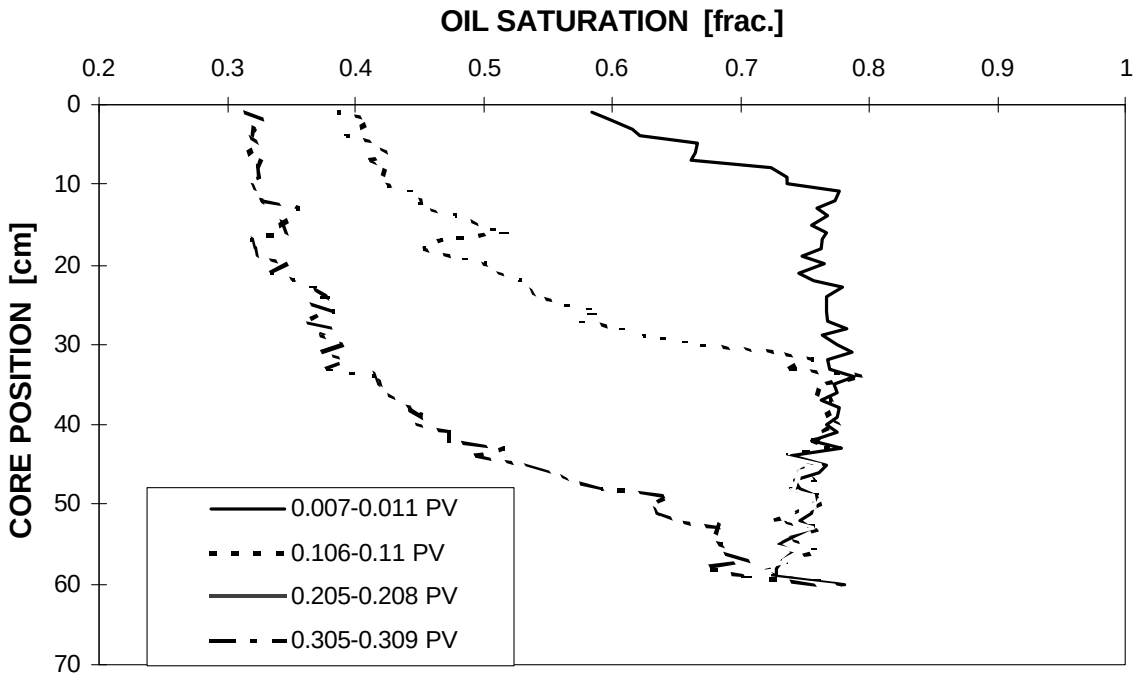

Figure 3a. Saturation profiles, q = 0.85*q_c

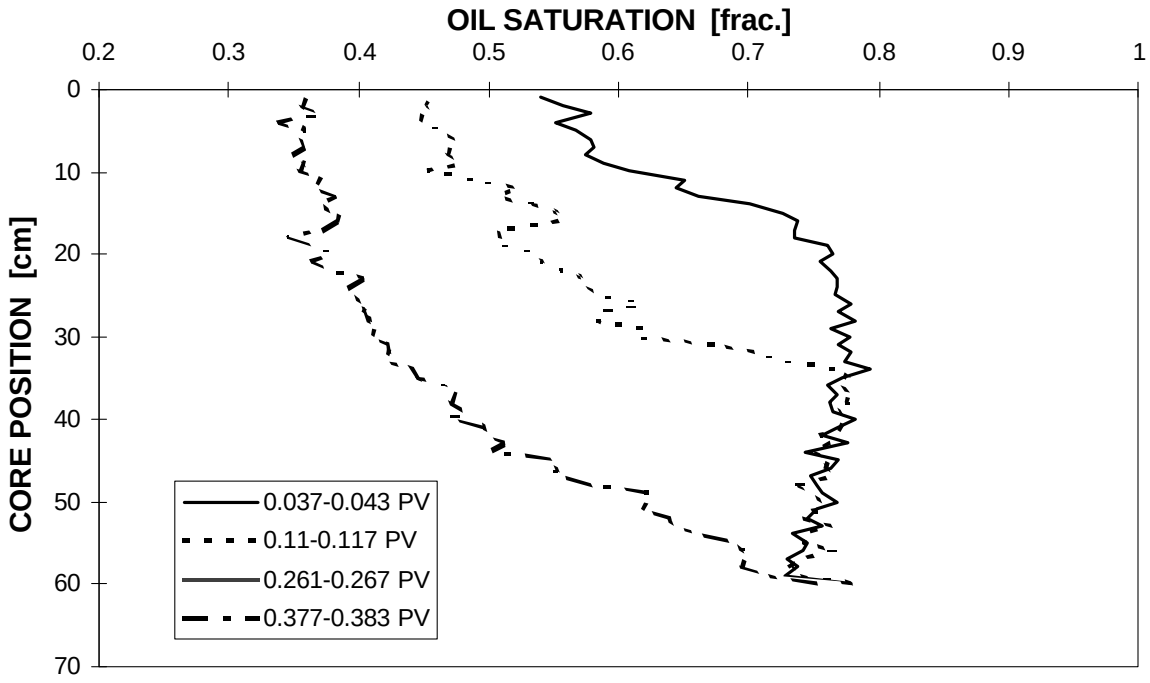

Figure 3b. Saturation profiles, q = 1.43*q_c

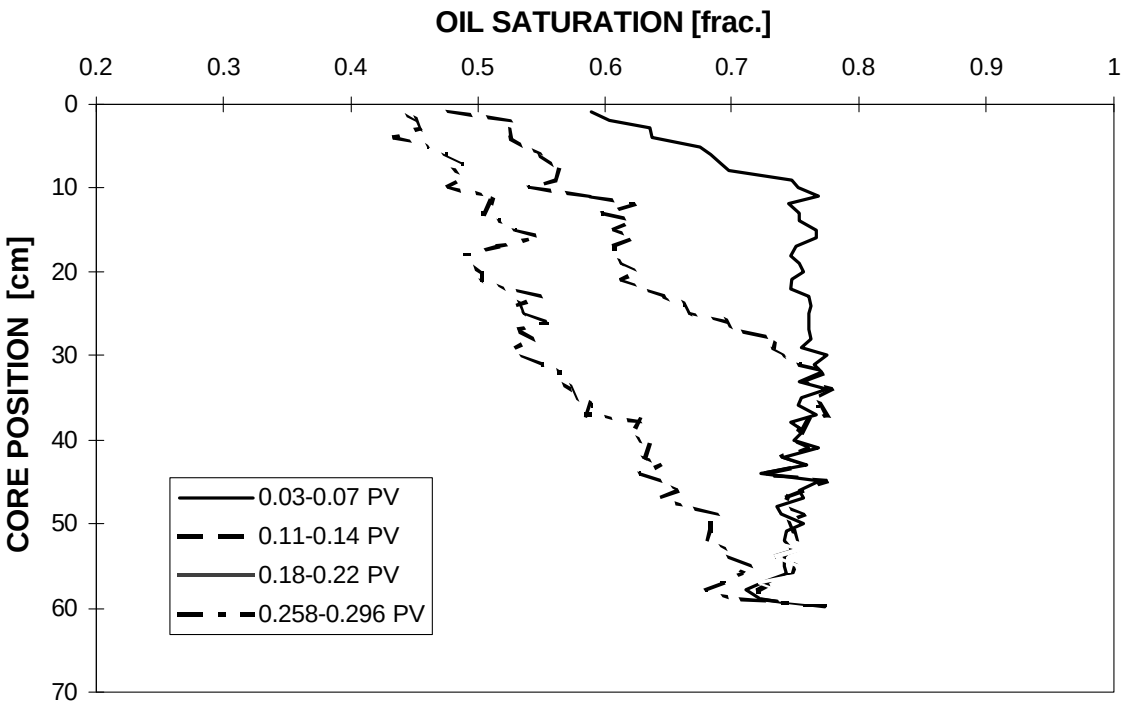

Figure 3c. Saturation profiles, q = 8.0*q_c

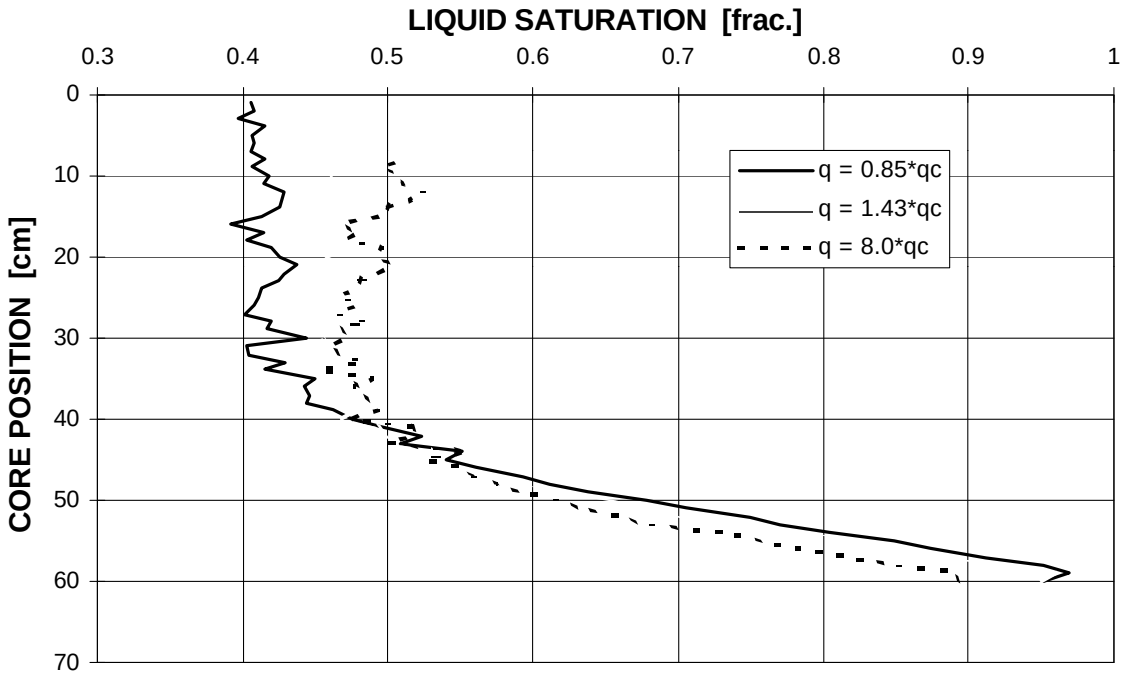

Figure 4. Saturation profiles at end of gas injection

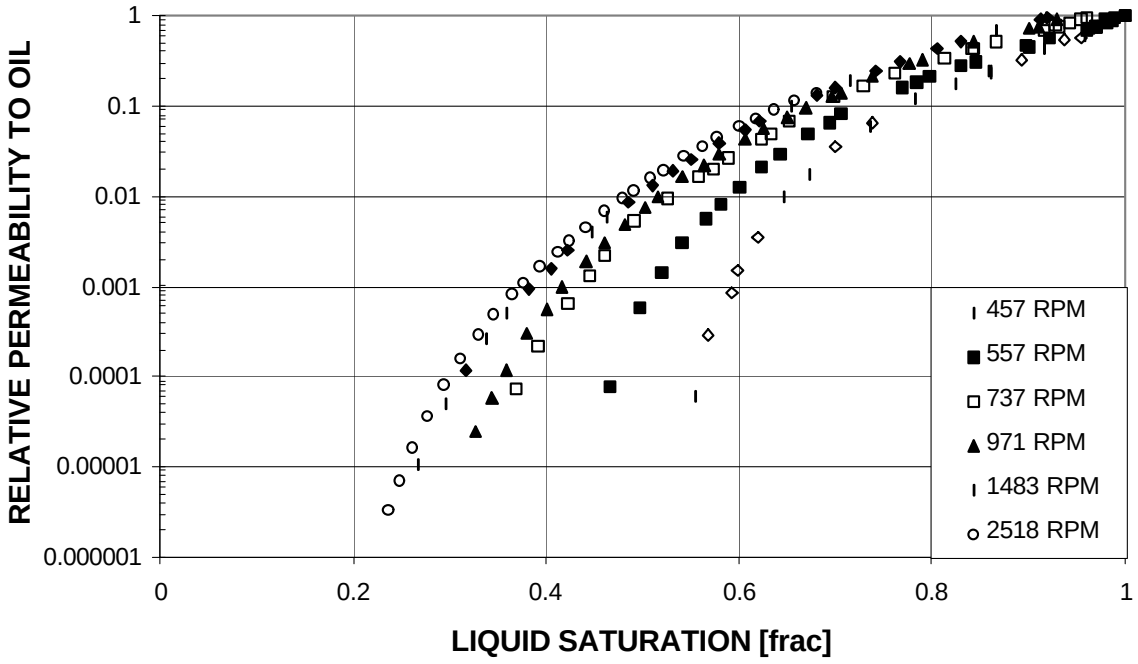

Figure 5a: Oil relative permeability from gas drainage in centrifuge, low permeability core

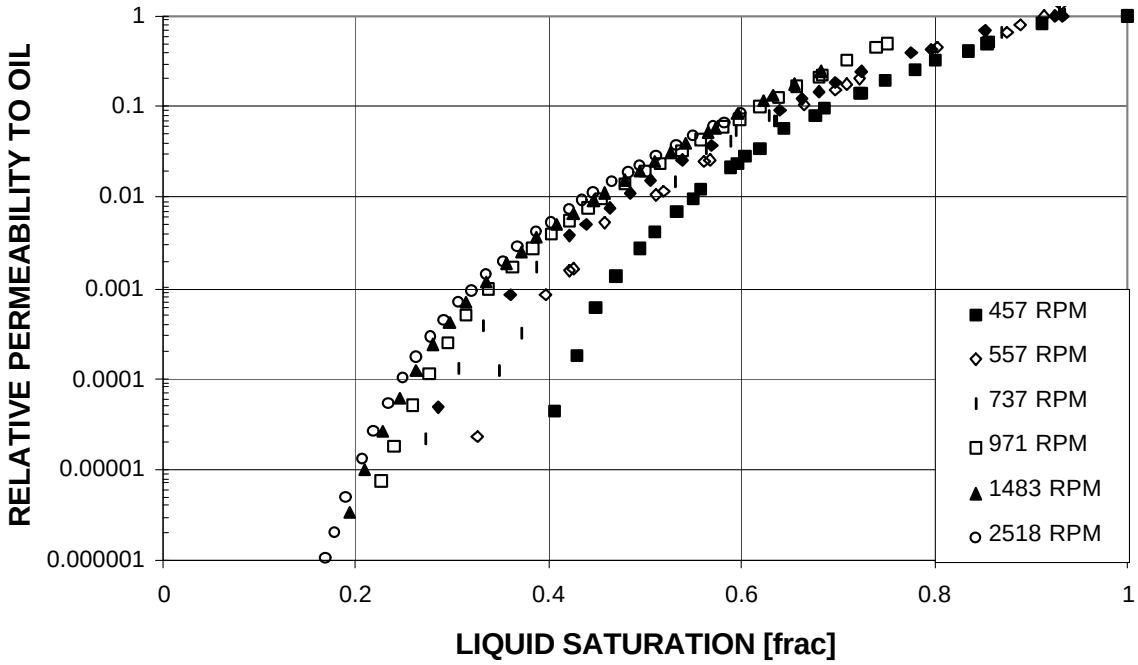

Figure 5b: Oil relative permeability from gas drainage in centrifuge, medium permeability core

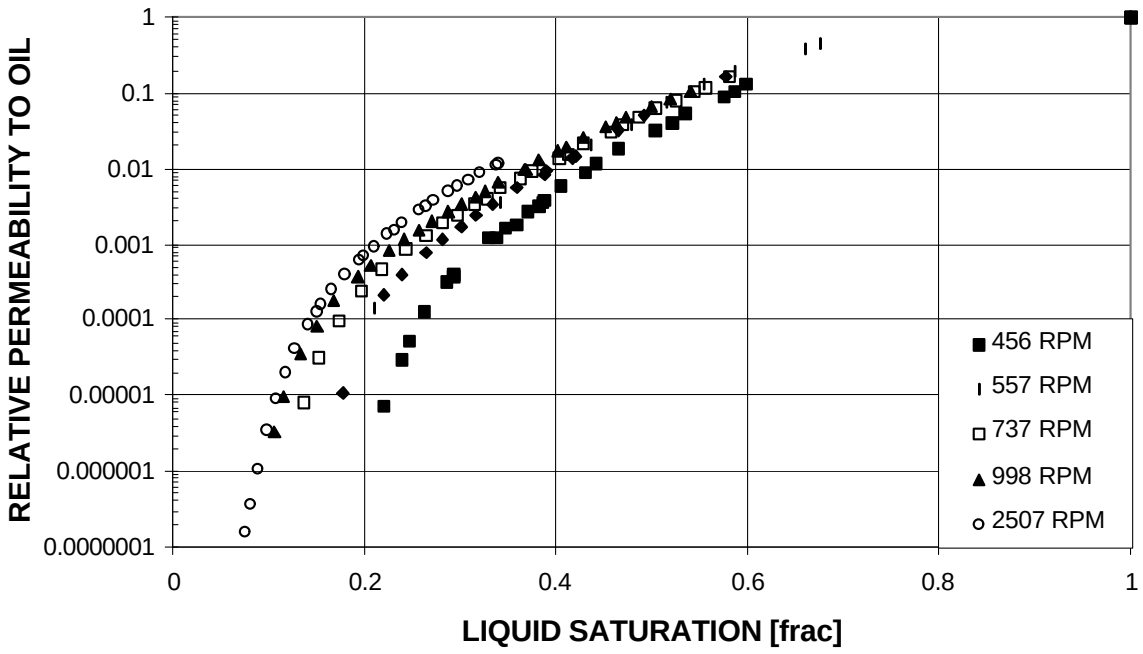

Figure 5c: Oil relative permeability from gas drainage in centrifuge, high permeability core

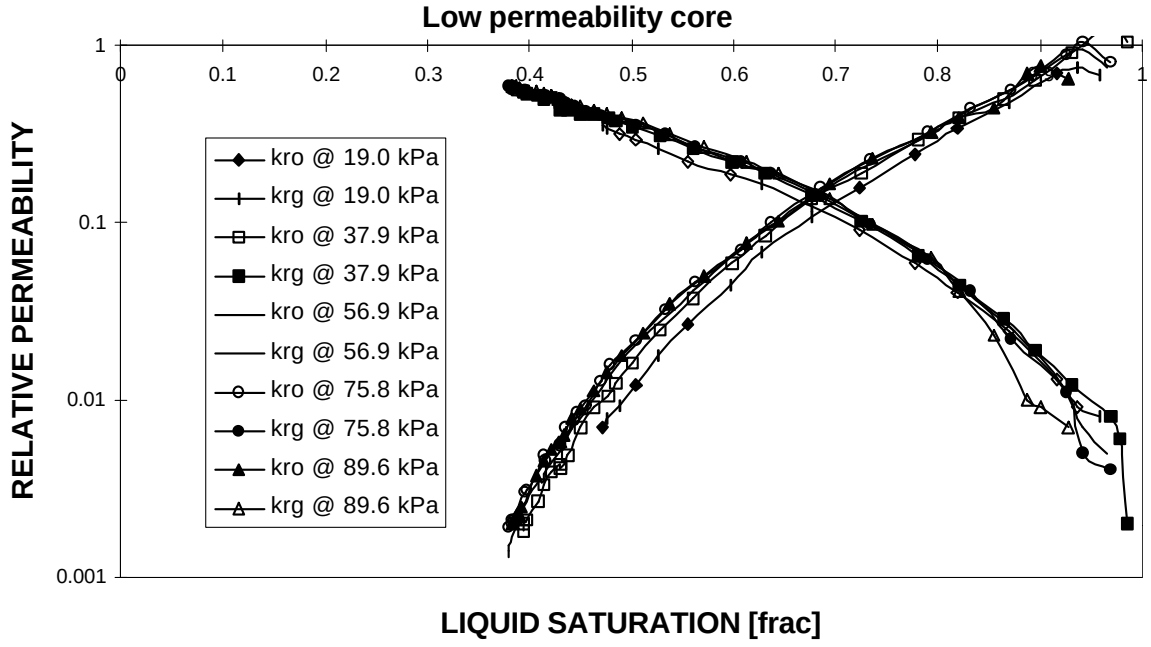

Figure 6a: Relative permeability from constant pressure gradient, low permeability core

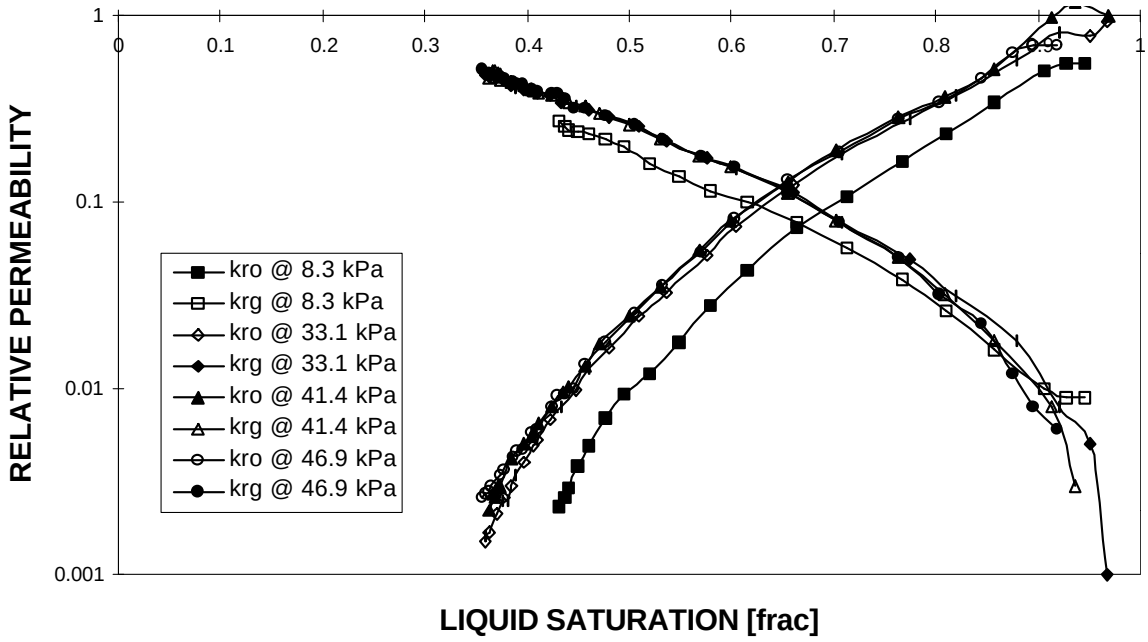

Figure 6b: Relative permeability from constant pressure gradient, medium permeability core

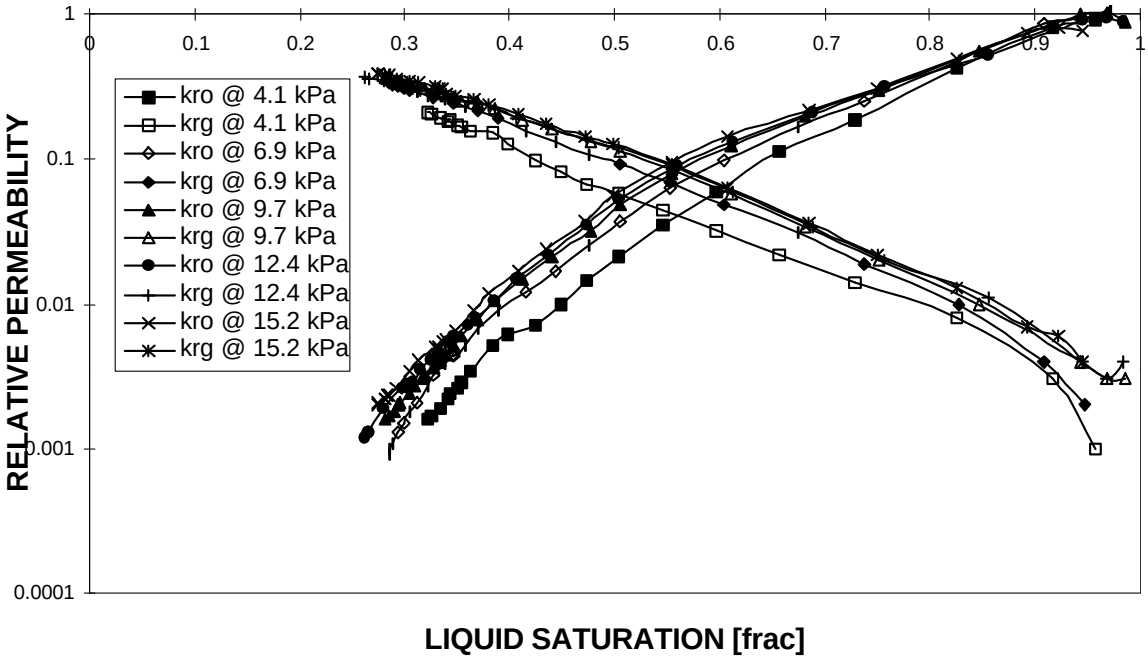

Figure 6c: Relative permeability from constant pressure gradient, high permeability core

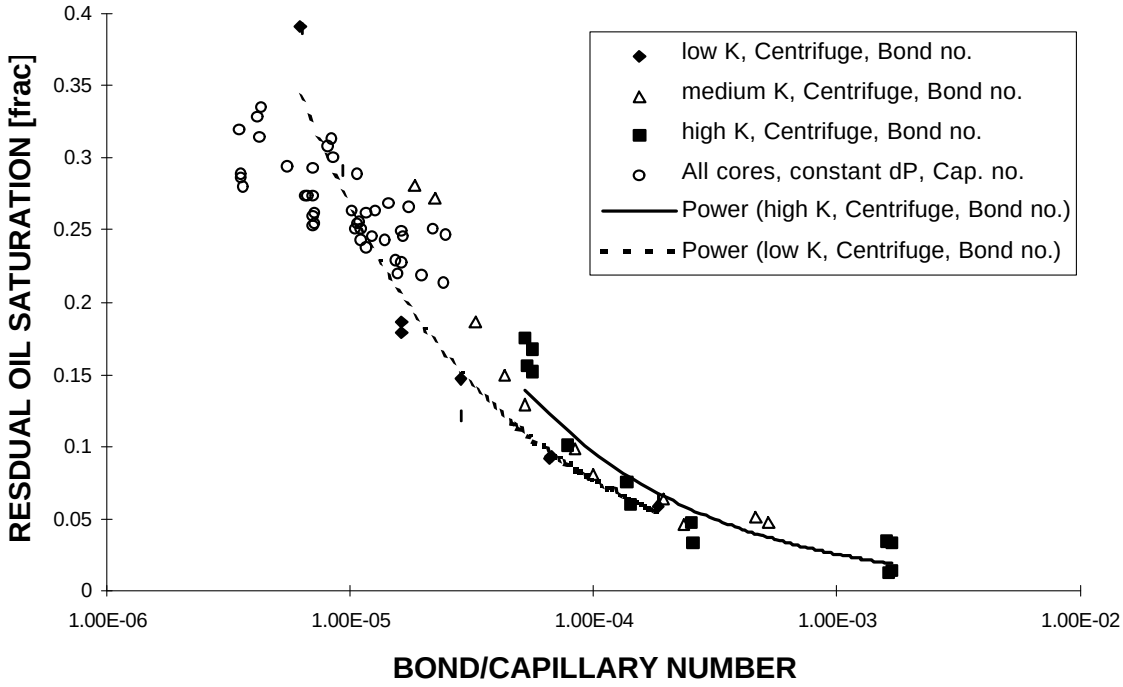

Figure 7. Remaining oil saturation versus Bond/Capillary number from centrifuge and constant pressure gradient experiments.

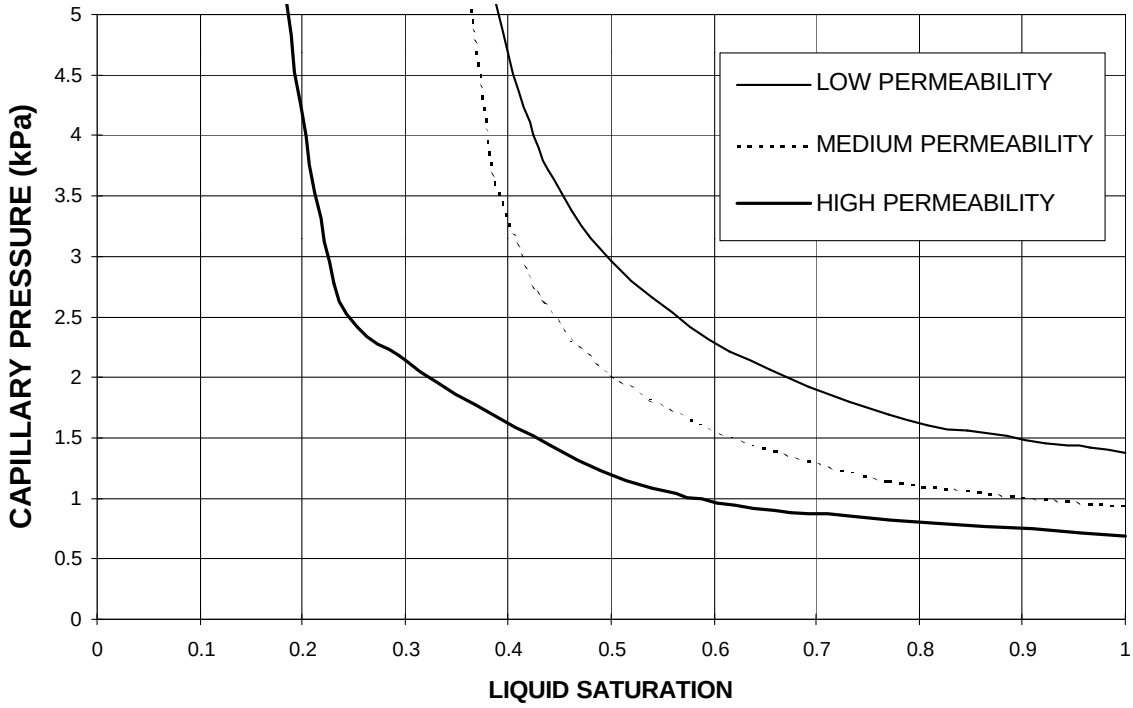

Figure 8. Capillary pressure curves

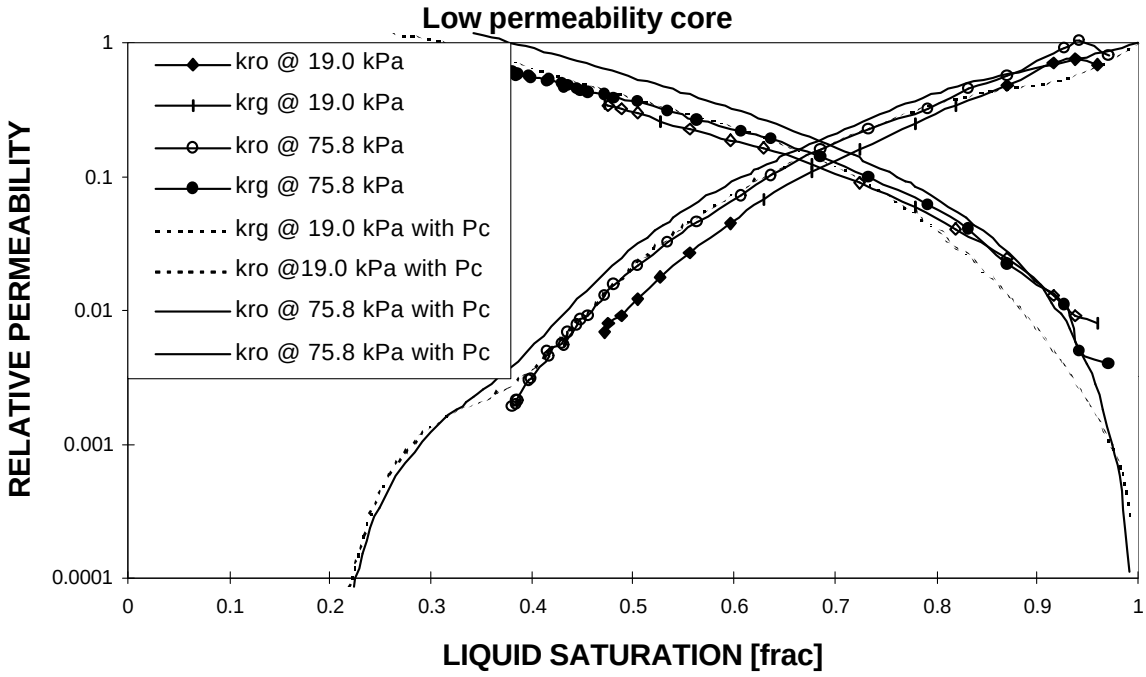

Figure 9. Relative permeability from constant pressure gradient experiment, with Pc simulation

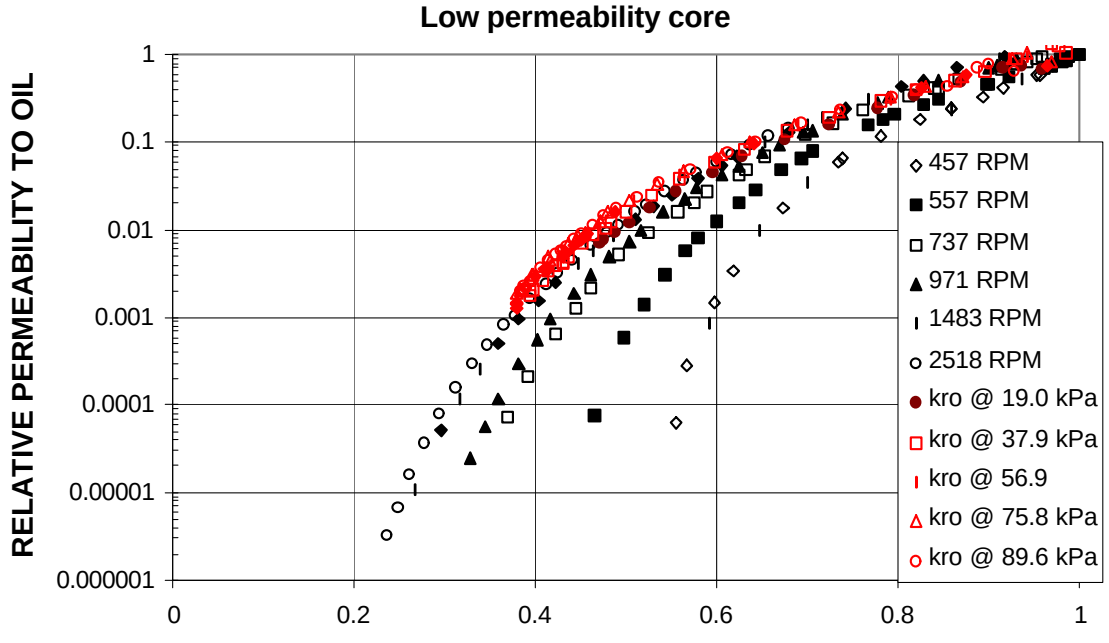

Figure 10. Oil relative permeability on low permeability core, centrifuge and constant pressure gradient.

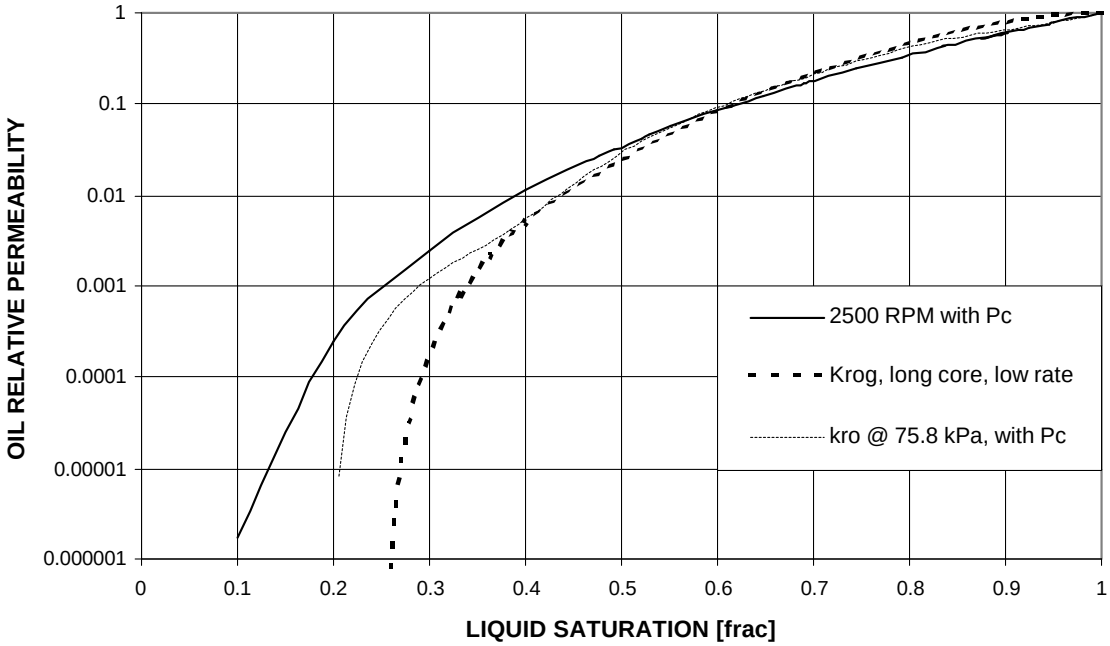

Figure 11. Comparison of oil relative permeability, low permeability core

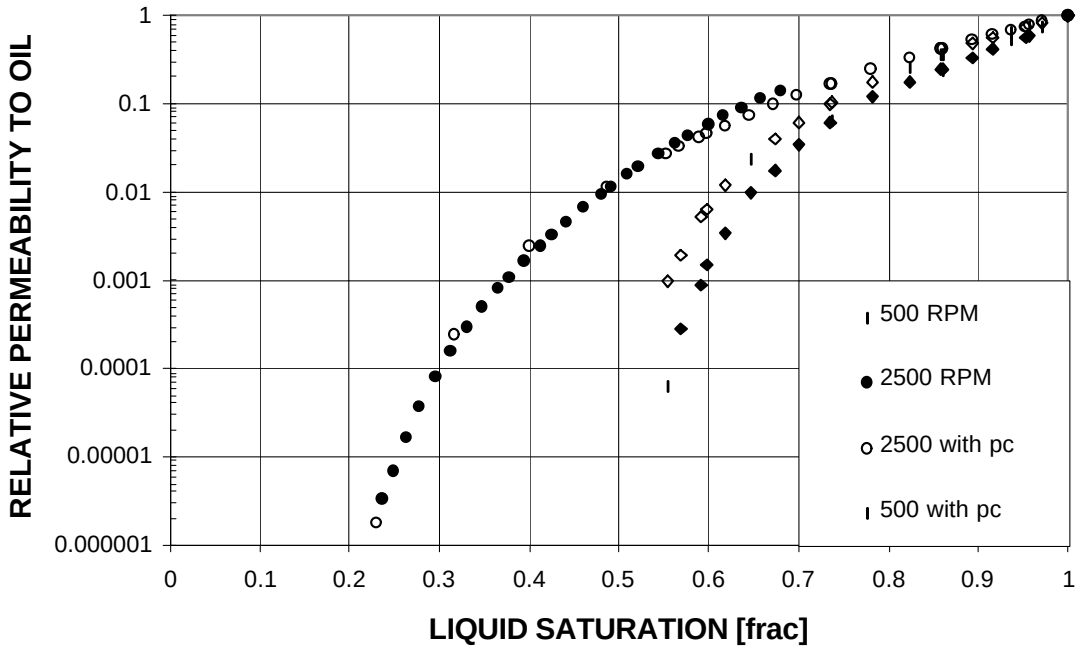

Figure 12. Oil relative permeability from centrifuge with Pc from low permeability core

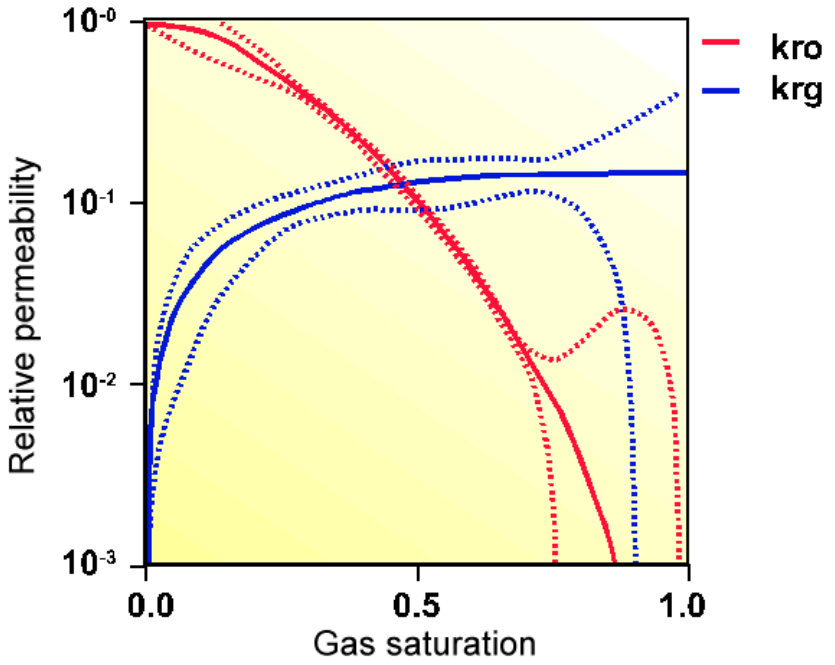

Figure A3. Estimated relative permeability from long core, low-rate experiment with confidence regions

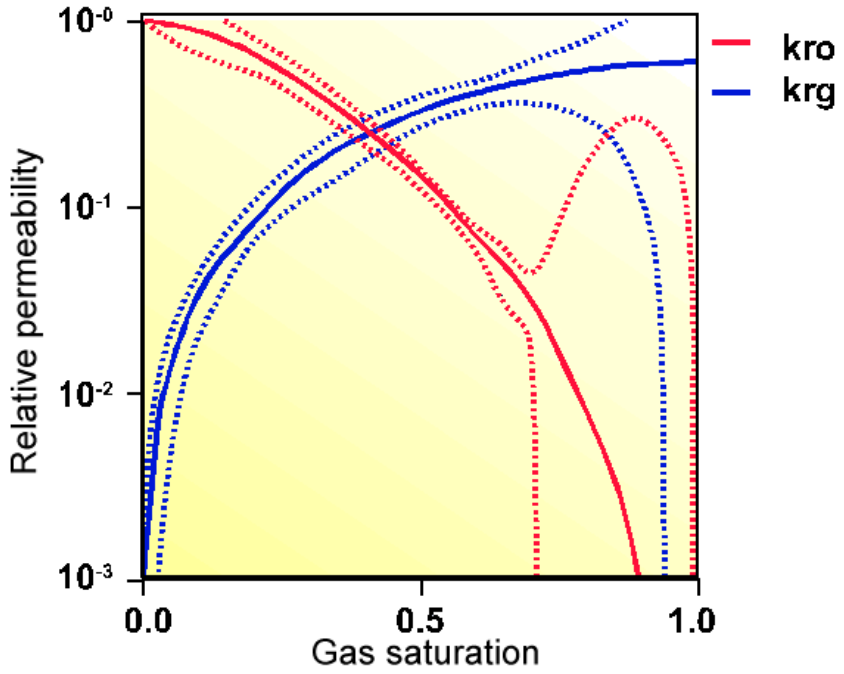

Figure 14. Estimated relative permeability from long core, high-rate experiment with confidence regions

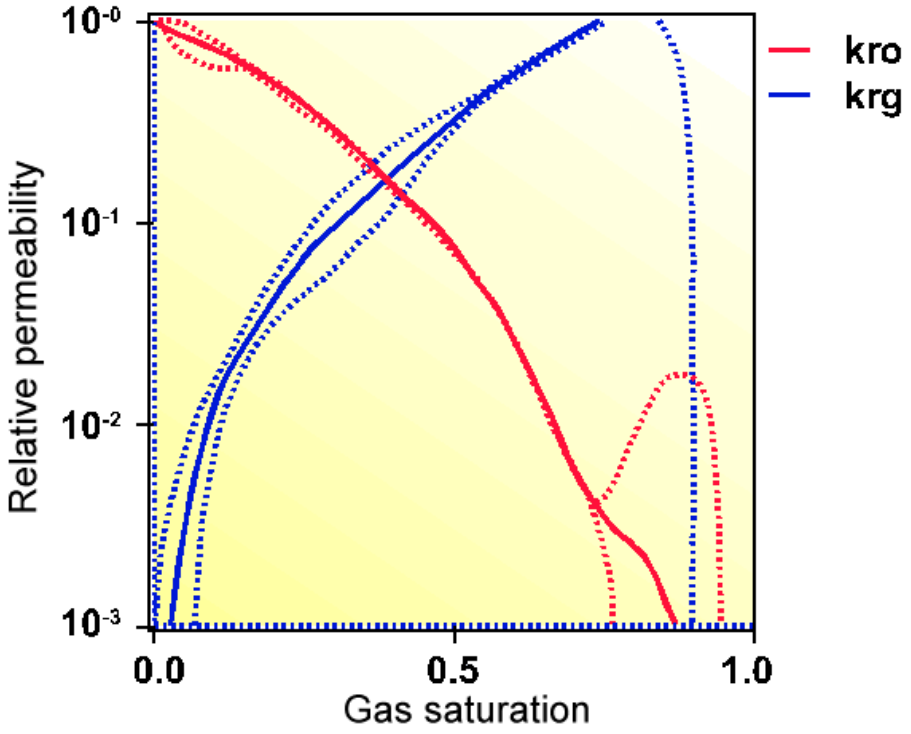

Figure 15. Estimated relative permeability from constant pressure experiment, 75.8 kPa drive pressure, with confidence regions